Metrology of steel micro-nozzles using X-ray microtomography

Delphine Lazaro [1], Samuel Legoupil [1], Grégory Blokkeel [2], Benoît Jeanne [2]

[1] Commissariat à l'Energie Atomique, Laboratoire Intégration et Architecture des Systèmes, F-91191 Gif-sur-Yvette, France; Phone: +33 1 69 08 52 81, Fax: +33 1 69 08 60 30; e-mail: delphine.lazaro@cea.fr, samuel.legoupil@cea.fr

[2] PSA Peugeot-Citroën, F-78943 Vélizy, France; e-mail: gregory.blokkeel@mpsa.com, benoit.jeanne@mpsa.com

Abstract

The development of direct-injection (DI) engines opened the way to even more fuel-efficient and cleaner engines. However, their optimization requires precise understanding of phenomena involved in the injection and atomization processes. The micronozzle internal structure plays a key role by favouring cavitation inside the micronozzle, which highly influence the fuel spray development. In the present study, X-ray microtomography was used to determine the 3D geometry of two micronozzles, one being cavitant and the other non-cavitant. Experiments were performed using a microfocus X-ray source coupled to a CMOS flat-panel detector. Two-dimensional images were acquired at different 360 angles and reconstructed using a 2D fan-beam reconstruction algorithm. The micronozzle surface was extracted from reconstructed images after segmentation. The obtained spatial resolution allowed to estimate micronozzle diameter values with a standard deviation of 5 µm, but was too poor was not to estimate accurately the curvature radius of the orifices. Micrometric imaging techniques, such as propagation-based phase-enhanced imaging or local tomography, should be investigated.

Keywords: fuel atomization; microtomography; reconstruction; metrology; direct injection

1. Introduction

International competition, environmental concerns and research towards better engine efficiencies continuously make automotive industries worldwide improving engine design. Direct-injection (DI) systems were developed as a very promising technology which enables an atomisation of the liquid fuel directly into the combustion chamber, leading to a better quality of fuel spraying and an accurate control of injected quantities. Moreover, higher injection pressures (> 150 MPa) and smaller orifice diameters of the nozzles (< 150 µm) can now be reached thanks to recent technological advances in fuel-injector nozzle manufacturing. These improvements allow the development of diesel DI engines even more fuel-efficient, cleaner, silent and powerful. Several complex and interdependent phenomena are involved during the injection and the spray atomization. The precise understanding of all these phenomena, as well as their interactions and the parameters influencing them, remain key issues to fully optimized the different DI systems regarding combustion efficiency and pollutant formation [1].

This study takes place in the framework of the EMPhASE project, which aims at characterizing thoroughly the whole chain of physical processes involved in the injection and the fuel spray atomization processes by performing both experiments and numerical simulations. Despite numerous experimental studies [2], phenomena taking part within the nozzle and in the region very close to the nozzle exit are still misunderstood because these regions are small and optically dense, which limits quantitative experimental analysis. 1D and then 3D numerical models were thus developed to investigate these regions where experiment was made difficult. However, current numerical models do not take into account in details phenomena within the

nozzle, such as cavitation which is of great importance. Indeed, cavitation is due to high injection pressures and flow speeds within the nozzle and highly influences the features of the spray atomization. The size and shape of the nozzle were also shown to greatly modify flow speeds inside the injection orifices [3]. Innovative experimental methods (Mie diffusion-based and x-ray imaging, optical techniques, laser-induced fluorescence, …) were proposed in this project to study the atomization process, particularly in regions where difficult experimental conditions are met. These experimental data will then be used to improve and develop numerical models of the atomization. Another goal of the project is to quantify the influence of the nozzle geometry on the spray development and to implement this effect into numerical models. For this, two different geometries of nozzles were considered, on being cavitant and the other non-cavitant.
In this study, X-ray computed microtomography was proposed as a non-destructive 3D imaging technique to determine the micronozzle geometry, which will then be used as input data for computed fluid dynamics (CFD) of the fuel spray. The main challenge was to be able to discriminate the non-cavitant nozzle geometry from the non-cavitant, which implies to reach a spatial resolution of about 5-10 µm in the reconstructed images. This performance was obtained by coupling a microfocus x-ray generator with a flat-panel detector with 50 µm pixel size with an appropriate magnification ratio. In a recent work [4], authors reported the use of X-ray propagation-based phase-enhanced microimaging to determine the metrology of steel micronozzles. The authors succeeded to detect defects non visualized by any other non-destructive techniques, with a typical size of 3 to 5 µm. The main drawback of this method is that it requires an x-ray synchrotron source facility. X-ray micromotomography allows ease-of-use and is a more convenient and cheaper technique.
In the first section of this paper, the geometry of the two studied micronozzles was presented, as well as the experimental set-up and the experiments. In the second section are detailed the different image processing steps applied to the projections images to finally extract the nozzle surface (image correction, reconstruction, segmentation and surface extraction). In this section are also given the parameters of interest measured from the nozzle surface. Results are then presented and discussed in the third section.

2. Methods

2.1 Experiments

Experiments were performed using our X-ray microtomography system which consists of a microfocus x-ray generator, a sample holder mounted on a computer-controlled translation and rotation systems and a CMOS flat-panel detector. These components are shown on Figure 1a.

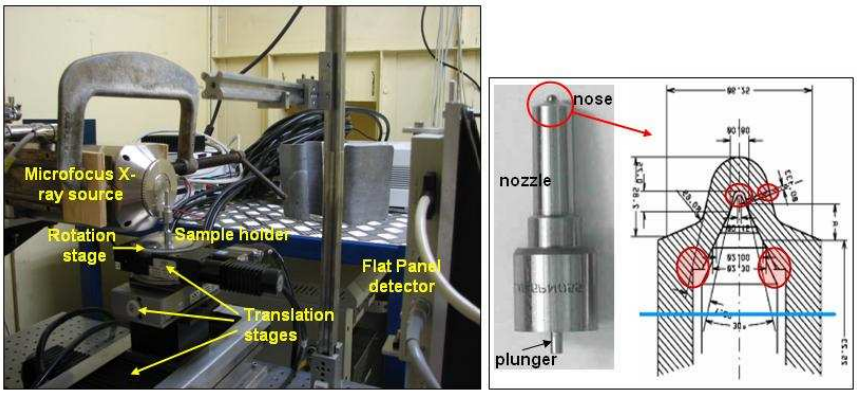

Figure 1. (a) Picture of the X-ray microtomography set-up. (b) Components of a nozzle (left) and scheme of the nozzle nose, with the regions to investigate in red (right)

The microfocus x-ray source (Feinfocus, Germany) is a tube equipped with a 5 µm thick tungsten target deposited on a 250 µm thick diamond substrate. This source is characterized by a small focal spot size, varying from 1 µm to 15 µm depending on the applied tube power. The maximum tube voltage and power are 160 kV and 10 W. For these experiments, the X-ray tube voltage and power were determined using MCNP-X Monte Carlo simulations and were finally set to 120 kV and 3.3 W, respectively. The tube was operated with a focal spot size of 7 µm at 120 kV, which limits spatial blurring.

The detector is a CMOS flat-panel detector (C7942, Hamamatsu, Japan) consisting in a CsI:Tl scintillator structured in 300 µm thick needles and a 2400 × 2400 matrix of transistors and photodiodes with a pixel pitch of 50 µm. The optical photons generated by the scintillator when irradiated by X-rays are converted to electrical charges in the readout photodiode array. The pixel size is 50 µm and the measured spatial resolution is 90 µm. The field-of-view (FOV) of the flat-panel is 12 cm × 12 cm. The detection efficiency is about 10% in the energy range of this application (120 kV).

The two micronozzles (Bosch, GmBh) (see Figure 1b) considered in this study were both made of steel and have 6 orifices equiangularly spaced, with a cylindrical section. They only differed by the orifice size and shape: one of the micronozzles presented cylindrical shape orifices while the other presented conical shape orifices, with a decrease of the diameter at the orifice exit. This conical geometry favoured the development of cavitation phenomena. The blue line represented on Figure 1b limits the important region of interest (ROI), in which the 3D internal structure of the micronozzles had to be determined for further Computed Flow Dynamic (CFD) computations. Red circles indicate ROI where a spatial resolution of at least 5 µm is required.

The spatial resolution in the acquired images is set by the magnification ratio, defined as the ratio between the source-to-object distance (SO) to the source-to-detector distance (SD). A magnification ratio of 29 (SO = 1.2 cm and SD = 35 cm) was chosen to image the top part of the nozzle nose, where ROI needed to be imaged with a spatial resolution of at least 5 µm. The pixel size in the acquired images was thus 1.7 µm. Because of the limited size of the detector FOV, the huge amount of experimental data generated, and taking into account that the other parts of the nozzles were of less importance, we chose to reduce this magnification ratio to 13 (SO = 2.55 cm and SD = 35 cm) so that the

bottom part of the nozzle nose could be imaged in one single acquisition. The pixel size in the acquired images was thus equal to 3.75 µm.
Finally, two tomographic acquisitions were performed for each micronozzle, one to determine the 3D geometry of the top part and the other to determine the 3D geometry of the bottom part. For each acquisition, 360 projections were taken each 1°: the integration times were set to 10 s and 20 s for the top part and bottom part acquisitions, respectively.

2.2 Image processing

2.2.2 Tomographic reconstruction

The acquired projections were first corrected for hot and dead pixels, dark current (measured in the absence of X-rays) and flat field (image acquired with X-rays in the absence of the sample). They were also corrected for beam-hardening before being converted into sinograms. Sinograms were then centred on the system axis of rotation to prevent additional spatial blurring on the reconstructed slices.
Since the cone beam Feldkamp reconstruction algorithm is computationally intensive and the amount of projection data was huge (about 20 Go for one tomographic acquisition), the 2D fan-beam filtered backprojection algorithm [5] was chosen to reconstruct the sinograms. The Ramp filter was applied for filtering the sinogram data before backprojection (cut-off frequency of 0.5 $pixel^{-1}$). In the nozzle top part, 1300 slices of 2048 × 2048 voxels were reconstructed with a thickness of 1.3 µm and a voxel size of 3.2 µm × 3.2 µm. In the nozzle bottom part, 1300 slices of 1024 × 1024 voxels were reconstructed with a slice thickness of 2.9 µm and a voxel size of 13.5 µm × 13.5 µm. In order to speed up the reconstruction time, slice were reconstructed one by one by splitting reconstructions into 3 computers, each one equipped with dual CPUs (BI-X, 64 bits, 3.2 GHz, 2Go RAM). A total reconstruction time of 77 hours was thus reached for one micronozzle.

2.2.3 Segmentation and surface extraction

The two set of reconstructed slices (top and bottom parts of the micronozzle) were processed so that their binning were identical and were merged, leading to a final voxel volume of 3.2 × 3.2 × 3.2 μm^3. A threshold-based segmentation method implemented in the AMIRA software (TGS Mercury, USA) was used to segment slices into air and steel. Slices were stacked to form separated 3D volumes for the nozzle and the plunger, from which surfaces were extracted. Surfaces were then stored in the STL format, e.g the surface is described by a list of triangular facets. A number of 1 million facets was chosen to describe surfaces with enough accuracy in spatial resolution.

2.2.4 Metrology

Diameters at the entrance (noted d_{in}) and at the exit (noted d_{out}) of the orifices were measured to discriminate the non-cavitant to the cavitant geometry. For each micronozzle and for each orifice, both diameters were measured twice in the axial and transaxial plans. Average values and associated standard deviations were then calculated for d_{in} and d_{out} and compared to nominal values reported by the manufacturer.

For the cavitant micronozzle, it is suspected that a specific surface treatment (electro erosion) was applied to erode the orifices at the exit and thus modified the curvature radius at the exit. The presence of this curvature radius at the orifice exit was qualitatively investigated by comparing reconstructed slices of the non-cavitant and the cavitant micronozzles in the region where the orifices end.

3. Results and discussion

2.1 Tomographic reconstruction, segmentation and surface extraction

Some reconstructed slices are shown on Figure 2 and Figure 3 for the top and the bottom parts of the non-cavitant micronozzle, respectively.

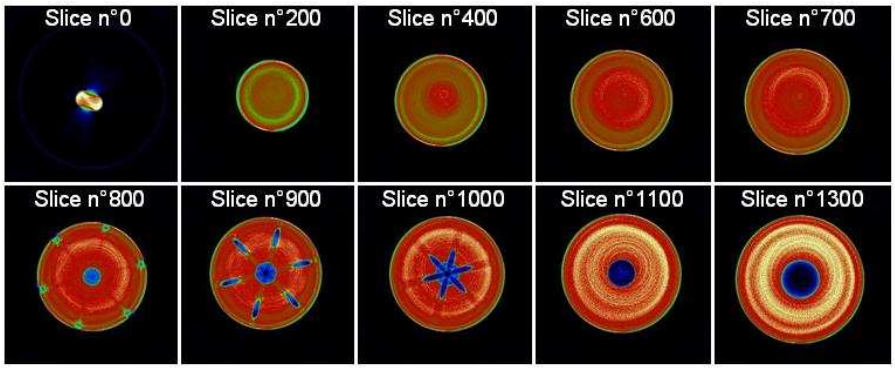

Figure 2. Reconstructed slices of the nozzle top part at different altitudes

Orifices are clearly visualized from slice n°800 to slice n°1100. From slice n°0 to slice n°400, reconstruction artefacts due to the use of a 2D fan-beam reconstruction algorithm instead of a 3D cone-beam algorithm can be seen and highly deform the shape of the reconstructed nozzle.
Both the nozzle and the plunger can be seen on Figure 3, from slice n°200 to slice n°500.

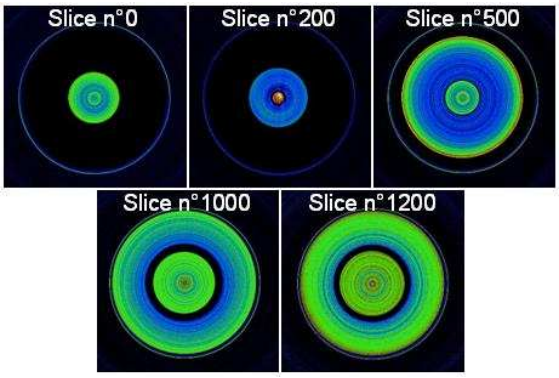

Figure 3. Reconstructed slices of the nozzle bottom part at different altitudes

Segmentation for one slice and surface extraction steps are shown on Figure 4.

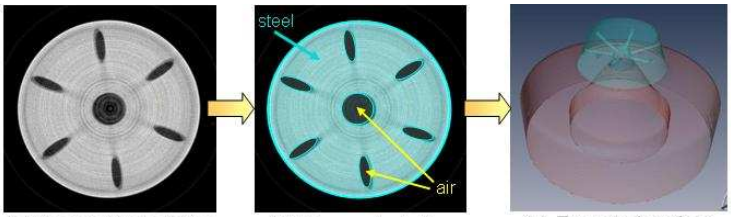

Figure 4. (a) Reconstructed slices, (b) the same slice after segmentation (steel in blue and air in grey) and (c) surface of the nozzle extracted from the stack of slices

The reconstructed slice (Figure 4a) is segmented into air and steel (Figure 4b), which are represented in blue and grey respectively. The blue line gives the surface boundary between air and steel. By stacking all the segmented slices, the surface of the volume can be extracted (Figure 4c).

2.2 Metrology

Measured and reference values reported by the manufacturer of the orifice entrance and exit diameters are compared in Table 1.

Table 1. Measured and reference values of the diameters at the entrance and the exit of the orifices, for the non-cavitant and the cavitant micronozzles.

Metrology method	Non-cavitant nozzle		Cavitant nozzle	
	d_{in} (µm)	d_{out} (µm)	d_{in} (µm)	d_{out} (µm)
X-ray microtomography	126.6 ± 3	129.6 ± 3	144.1 ± 3	132.9 ± 4
Manufacturer	141.2 ± 1.6	140.9 ± 0.2	140.8 ± 1.7	125.0 ± 0.4

Relative differences between measured and reference values are about 10% and 8% for d_{in} and d_{out} respectively for the non-cavitant micronozzle, and about 3% and 6% for d_{in} and d_{out} respectively for the cavitant micronozzle. For the cavitant micronozzle, the d_{in} value was estimated by measuring the diameter at the orifice entrance from the internal side. Measured values with x-ray microtomography are thus close to the values reported by the manufacturer and are given with a standard deviation varying between 3 and 4 µm, which means that x-ray microtomography can be considered as a valuable metrology method to image details in the range of 5 µm.
Reconstructed slices of the non-cavitant and the cavitant micronozzles are compared on Figure 5 in the region where the orifices end. It can be seen that the curvature radius is different between both micronozzles and seems to be more important for the cavitant micronozzle. However, the lack in spatial resolution in this region makes difficult the accurate measurement of this curvature radius.

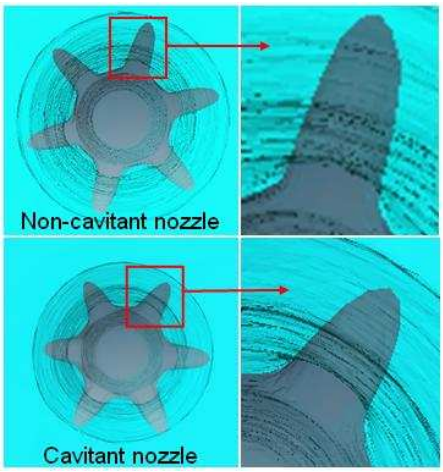

Figure 5. Reconstructed slices for the non-cavitant nozzle (top) and the cavitant nozzle (bottom) in the region where the orifices end. Associated zoomed images are shown on the right

4. Conclusion

We have demonstrated in this study that X-ray computed microtomography was a valuable non-destructive metrology method to investigate 3D internal geometry of micronozzles, e.g very absorbing samples. Using this method, orifice diameters of micronozzles could be estimated with a spatial resolution of about 5 µm, which allowed to discriminate non-cavitant micronozzle geometries from cavitant geometries. However, these results have also shown the limitations of this method when imaging much smaller details in the micronozzle specific regions, as the curvature radius. A micrometric spatial resolution would be thus required and could be reached by using other imaging techniques, among which propagation-based phase-enhanced imaging using a synchrotron source [3] or local tomography. This latter method is currently under study in our lab.

Acknowledgements

This work was funded by the French Research National Agency (ANR) in the framework of the PREDIT EMPhASE project. The authors wish to acknowledge Conseil Général de l'Essonne for its participation in the funding of the microtomography set-up.

References

1. F Zhao, M C Lai and D L Harrington, 'Automotive spark-ignited direct-injection gasoline engines', *Prog. Energy Combust. Sci.*, Vol. 25, pp 437-562, 1999.
2. H Chaves, M Knapp, A Kubitzek, F Obermeier and T Schneider, 'Experimental study of cavitation in the nozzle hole of Diesel injectors using transparent nozzles', *SAE 950290, 23, 29, 31*, 1995.
3. W Bergwerk, 'Flow pattern in Diesel nozzle spray holes', *Proc. Of the Inst. Of Mech. Engineers*, Vol. 173, n°25, pp 655-660, 1959.

4. W K Lee, K Feeza and J Wang, ‘Metrology of steel micronozzles using x-ray propagation-based phase-enhanced microimaging’, *Appl. Phys. Letters*, Vol. 87, 084105, 2005.
5. A Kak and M Slaney, ‘Principles of Computerized Tomographic Imaging’, *IEEE Press, New York*, 1987.